Check for updates

Preparation, characterization and application of CS@PDA@Fe₃O₄ nanocomposite as a new magnetic nano-adsorber for the removal of metals and dyes in wastewater†

Xingjing Zhang, Baohe Li, Xiaoqian Han [ID] * and Nong Wang

This study aimed to develop a novel magnetic chitosan/dopamine/Fe₃O₄ nano-adsorber (CS@PDA@Fe₃O₄) for the removal of heavy metal ions and organic dye molecules from aqueous solution. CS@PDA@Fe₃O₄ was prepared by surface modification of PDA/Fe₃O₄ nanoparticles with chitosan using IPTES as the cross-linker. The surface structure, composition, and properties of the CS@PDA@Fe₃O₄ nano-adsorber were characterized by elemental (EDS), spectroscopic (XRD, XPS, and FT-IR), magnetic intensity (VSM), surface and morphological (TEM and SEM) analyses. In order to study its adsorption behavior, equilibrium and kinetics studies were carried out through batch experiments. Additionally, the influences of the pH value, initial concentration, adsorbent dose, and contact time were also evaluated. The CS@PDA@Fe₃O₄ nano-adsorber exhibited high adsorption capacity especially for Cu(II), with a maximum adsorption capacity of 419.6 mg g⁻¹. The experimental data were well described by the Langmuir isotherm kinetic models.

1. Introduction

A growing social and economic concern is water contamination due to the discharge of many dyes and heavy metal ions into the environment, which causes a potential threat to human health and the environment.[1,2] As everyone knows, heavy metal ions and most of the dyes are very poisonous or strongly oncogenic, and may cause bad effects to people's brains, lungs, and kidneys.[3] Therefore, it is particularly important to treat wastewater with a feasible and appropriate method.[4] The traditional ways such as electrochemical precipitation,[5] sorption,[6] reduction,[7] advanced oxidation,[8] etc. have been used to remove pollutants from water. In all technologies, the adsorption method has the advantages of low cost, and being green and environmentally friendly for the elimination of pollutants in water.[9] Various adsorbents have been reported for the treatment of metal ions and dye-contaminated water: activated carbon, zeolites, and clay minerals, which have disadvantages such as low adsorption abilities, narrow application scope, and difficult recovery problem.[10] New materials modified by natural adsorbents for easy adsorbent recovery have received extensive attention in recent years.[11]

Chitosan (CS), as the second most abundant natural polysaccharide after cellulose, has a large number of hydroxyl and amino functional groups in its chain moiety and exerts outstanding ability to interact with a wide variety of molecules by physical and chemical forces.[12] Therefore, it can be used for wastewater treatment.[13–15] However, the solubility of chitosan in an acidic environment limits its further application.[16] Due to using glutaraldehyde as a crosslinking agent in the traditional method, the amino content of chitosan decreased sharply, which affected the adsorption property. Therefore, we introduce dopamine as a new cross-linking agent for surface modification or modification.[17,18]

Dopamine (DA), a protein-based biomaterial that is found in the tentacles of mussel sea creatures, has abundant functional groups such as catechol groups, amine groups, and aromatic moieties. Hence, it can easily adsorpt heavy metal ions and toxic organic pollutants through chelation and π–π stacking interactions.[19,20] Furthermore, it has some advantages of easy processing, in a one-pot preparation method and chemical versatility, which proved to be a powerful tool for the removal of environmental water pollutants.[21,22]

In this study, a new, low-cost, nano-adsorber with the increased number of adsorption sites was developed. This new biopolymer adsorbent is a chitosan derivative, CS@PDA@Fe₃O₄ which was synthesized by assembling biomimetic polymer (PDA) and chitosan onto magnetic nanoparticles based on esterification reaction. The structure and properties of nano-adsorber were investigated by means of FTIR, SEM, TEM,

School of Chemical and Chemical Engineering, Lanzhou Jiaotong University, Lanzhou 730070, P. R. China. E-mail: hxqnv2011nv@163.com

XRD, VSM, and elemental analysis. The various studies in terms of isotherms and kinetics of adsorption of heavy metal ions and organic dye molecules were carried out. The effects of solution pH, dosage, initial concentration, and contact time on the adsorption process were optimized.

2. Experimental

2.1. Instruments and materials

$FeCl_2 \cdot 4H_2O$, $FeCl_3 \cdot 6H_2O$, sodium hydroxide (NaOH) and dopamine (DA) were purchased from Kaixin Chemical Industry. Trometamol was purchased from Zhongqin Chemical Reagent (Shanghai, China). Chitosan and γ-isocyanatopropyltriethoxysilane (IPTES) were purchased from Odofuni Biological Technology (Nanjing, China). Hydrochloric acid (HCl) was purchased from Chemical Factory (Beijing, China). Methylene blue (MB), Fuchsin basic (FB), Rhodamine B (RhB) were cationic dyes gained from Damao Chemical Reagent Factory (Tianjin, China). All other reagents were analytical grade and were used without any extra purification. Aqueous solutions at various concentrations were prepared from $HgCl_2$, were used as sources for Hg(II), $CuCl_2$, $PbCl_2$ were used as sources for Cu(II), Pb(II), respectively. The morphology was analyzed by scanning electron microscopy (SEM) (MIRN3, TESCAN, China) and (TEM) (Philip Tecnai20, Netherlands). Infrared spectroscopy was recorded by a Fourier transform infrared spectrometer (FTIR) (Vector22, Bruker, Germany). Vibrating-sample magnetometry (VSM) (Lake Shore7410, America). The types and contents of the elements were analyzed by an energy dispersive spectrometer (EDS) (FE SEM-4100, Hitachi Limited, Japan).

2.2. Synthesis of magnetite Fe_3O_4 nanoparticles

Magnetite Fe_3O_4 nanoparticles were synthesized by the method of coprecipitation according to reported investigation.[23] Briefly, $FeCl_3$ (8.15 g) and $FeCl_2$ (3.98 g) were weighed and dissolved in 25 mL deionized water respectively, the obtained mixture was mixed further stirred for 30 min at 60 °C, followed by NaOH (100 mL, 2 mol L^{-1}) for another 2 h. The produced mixture was washed in deionized water until neutral and dried at 70 °C for 12 h to obtain Fe_3O_4 nanoparticles.

2.3. Preparation of PDA@Fe_3O_4 nanocomposite

In a round-bottom flask, a solution of 300 mL of Tris–HCl buffer solution (pH = 8.5) was configured and then a certain amount of dopamine and magnetic Fe_3O_4 nanoparticles (1 g) was added. After sonication for 30 min, the reaction temperature was rose to 100 °C for 12 h to obtain the PDA@Fe_3O_4 nanocomposite.

2.4. Synthesis of CS@PDA@Fe_3O_4 nanocomposite

Chitosan (0.5 g) was added to anhydrous pyridine solution at 90 °C for 12 h. Add 0.5 mL IPTES in constant temperature stirring for 12 h. Then, PDA@Fe_3O_4 (0.5 g) was added, the stirring of mixture continued for 12 h. The black CS@PDA@Fe_3O_4 nanocomposite was separated using the magnetic decantation, washed with distilled water and alcohol thoroughly. The product was dried at 70 °C under the vacuum for 12 h.

2.5. Adsorption experiments

The adsorption was studied by batch methods that were carried out by placing CS@PDA@Fe_3O_4 (0.01 g) in series of flasks containing heavy metal ions or dyes in an aqueous solution (30 mL) with the desired initial concentration and pH. Then, the flasks were shaken in a thermostat oscillator at a certain temperature with the constant rate for a given time. The effects of operating variables such as pH value, contact time, initial concentration, and amount of adsorbent on the degree of adsorption were investigated. To investigate the effect of different solution pH on adsorption of heavy metal and dye, the desired pH range of the heavy metal and dye was adjusted from 1 to 7. The working concentration of heavy metal ions or dyes was 5.4 g L^{-1} for kinetic studies and 1.35–8.1 g L^{-1} for isotherm studies. Separate the magnetic microsphere CS@PDA@Fe_3O_4 from the solution and measure the absorbance of the solution before and after adsorption.

The amount of pollutant adsorbed per gram of the adsorber was calculated based on the following equation.[24]

$$\eta = \frac{C_0 - C_e}{C_0} \times 100\% \tag{1}$$

$$Q = \frac{V(C - C_e)}{M} \tag{2}$$

where η is the adsorption capacity (mg g^{-1}); C_0 and C_e are initial and equilibrium concentrations of the heavy metal ions or dyes (mg L^{-1}) in the testing solution (mg L^{-1}); V is the volume of the solution (L), and M is the weight of resin beads (g).

2.6. Recycling of CS@PDA@Fe_3O_4 nanocomposite

For the desorption experiment, the CS@PDA@Fe_3O_4 nanocomposite was separated, washed several times with absolute ethanol solution and distilled water, and used for the subsequent adsorption after drying at 70 °C under the vacuum for 12 h. In order to test the reusability of the CS@PDA@Fe_3O_4 nanocomposite, this adsorption–desorption cycle was repeated 6 times by using the same adsorbent.

3. Results and discussion

3.1. Characterization of CS@PDA@Fe_3O_4 biopolymer adsorbent

The nanoparticles of CS@PDA@Fe_3O_4 were synthesized in a three-step procedure. The CS@PDA@Fe_3O_4 was prepared using coating layer upon layer of Fe_3O_4, PDA and CS (Fig. 1). The adsorption principle of CS@PDA@Fe_3O_4 biopolymer adsorbent was that its chitosan layer molecule contains a large number of amino and hydroxyl groups, which formed mesh cage molecules by hydrogen bond, chelate many heavy metal ions and dye molecules. The prepared CS@PDA@Fe_3O_4 nanocomposite was characterized by various techniques such as FT-IR, vibration sample magnetometer (VSM), X-ray diffraction (XRD), transmission electron microscopy (TEM), scanning electron microscope (SEM), energy dispersive X-ray spectrometer (EDS), and X-ray photoelectron spectroscopy (XPS) analyses.
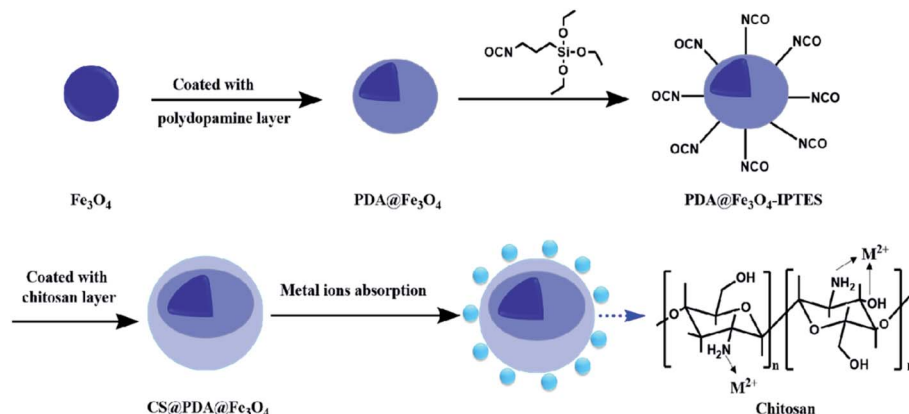
3.3 Effect of contact time, pH, adsorbent dose and initial concentration on properties of the CS@PDA@Fe$_3$O$_4$ nano-adsorber

The effect of contact time for the adsorption of heavy metals ions and organic dyes molecules by CS@PDA@Fe$_3$O$_4$ nano-adsorber at various intervals of time ranging from 10 to 120 min was investigated in the ambient experimental background. The results obtained were presented in Fig. 2a. The results confirmed that adsorption of metal ions and dyes has a consistent change rule: the initial stage of the rate of adsorption was faster and then gradually reduced and reached saturation.[13] Thus, 30 min, 70 min, 80 min, 100 min, 60 min, 60 min of contact time were respectively optimized for the adsorptive removal of Cu(ɪɪ), Hg(ɪɪ), Pb(ɪɪ), MB, FB and RhB.

The solution pH, as a critical operational variable, has a significant effect on the surface charge of the adsorption and the metal ion chemistry. For that, we investigated different processes when the pH ranged from 1 to 12 for heavy metal ions and dyes. The Cu(ɪɪ) cations tend to precipitate in the form of hydroxyl salts of Cu(ɪɪ) ions and FB has a large color change in alkaline solution, which has a detrimental effect on adsorption research. Therefore, the pH range of both of them was adjusted to 1–7. It can be seen from Fig. 2b that the removal rate of adsorbent on metal ions and dye molecules increases gradually with the increasing pH of the solution under acidic conditions. When the solution was neutral, the adsorption reaches saturation. The strongly acidic and alkaline conditions are not conducive to the effect of metal ions and dyes. The strong acidic solution containing a large number of H$^+$ will form a competitive relationship with metal ions for adsorption reduce the active sites, and there will be the partial dissolution of chitosan, thus reducing the adsorption performance. Besides, metal ions may be partially precipitated under basic conditions. In consequence, the optimum pH of heavy metal ions and dye molecules adsorption onto CS@PDA@Fe$_3$O$_4$ nano-adsorber was 7.

The adsorbent dosage is a key parameter for the sorption capacity of adsorbents. The dosage of CS@PDA@Fe$_3$O$_4$ nano-adsorber was varied in the range of 40–240 mg, in a fixed initial dyes and heavy metal ions concentration of 50 mg L^{-1}, the pH value of the solution was 7, at ambient experimental conditions. The effect of the adsorbent dosage on the adsorption of heavy metal ions and dye molecules were investigated, and the results were shown in Fig. 2c. With the increase of adsorption dose, the adsorption efficiency of heavy metal ions and dye molecules increased, which could be described based on the availability of active binding sites for the adsorbates on the surface of the adsorbent. When the amount of adsorbent increases to a certain value, the removal rate decreases after it remains stable. The reason could be that after the adsorption reaches equilibrium, part of the adsorbent will fall off from the adsorbent. Therefore, 100 mg of the CS@PDA@Fe$_3$O$_4$ nano-adsorber was chosen as the ideal dose for the following adsorption experiment.

The effects of different initial concentrations of dye molecules and heavy metal ions on their adsorption at optimal
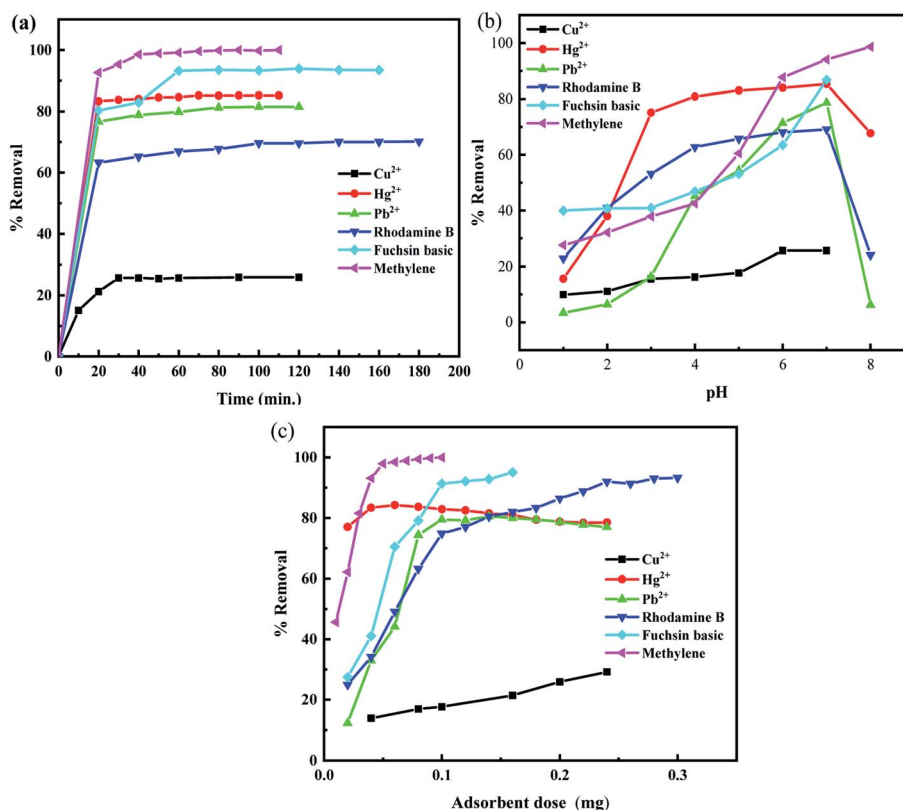

Fig. 2 Effect of (a) shacking time; (b) initial pH and (c) adsorbent dosage on the adsorption with the pH value of the solution was 7 at ambient experimental conditions.

contact time and pH were investigated. The relationship between adsorption amount and initial concentration was presented in Fig. 3. The adsorption of heavy metal ions and dye molecules showed a common change rule. As the initial concentration increases, the collision probability between the magnetic microspheres and the adsorbent increases, but when the initial concentration is large enough, the adsorption sites of the nano-adsorber are filled and saturated, and the removal rate reaches equilibrium or even decreases.

3.4 Adsorption kinetics

The adsorption kinetics are the crucial factors for determining the rate of the adsorption process, which provides essential data about the mechanism and rate of removal. Table 1 shows the kinetic profiles of heavy metals ions and organic dyes adsorption operation using CS@PDA@Fe$_3$O$_4$ as adsorbents, with time increasing. In order to investigate the removal mechanism of the adsorption of Cu(II), Hg(II), Pb(II) heavy metal ions and MB, FB, RhB dye molecules on CS@PDA@Fe$_3$O$_4$ nano-adsorber, the pseudo-first-order (3), pseudo-second-order (4) and intra-particle diffusion kinetic models (5) were employed to explore the experimental data.[29]

$$\log(Q - Q_t) = \log Q - \frac{K_1 t}{2.303} \tag{3}$$

$$\frac{t}{Q_t} = \frac{t}{Q} + \frac{1}{K_2 Q^2} \tag{4}$$

$$Q_t = K_{int} t^{0.5} + C \tag{5}$$

where K_1, K_2 and K_{int} are pseudo-first-order rate constant (min^{-1}), pseudo-second-order rate constant (g mg^{-1} min^{-1}) and intraparticle diffusion rate constant (mg g^{-1} min$^{-1/2}$) of adsorption, respectively. Q and Q_t are the adsorption capacity (mg g^{-1}) at equilibrium time and at time t (min), respectively. C (mg g^{-1}) is a constant of the intra-particle diffusion model.

The non-linear form of the reaction and diffusion-based kinetic parameters and their results were summarized in Table 1. Through the comparison and analysis of R^2 values in the table, the kinetic model. With the higher R^2 values of the pseudo-second-order kinetics model, the conclusion is drawn that the pseudo-second-order kinetics model was well simulated, which signifying that chemisorption dominated the adsorption process.

3.5 Adsorption isotherms

The adsorption isotherms are the crucial factors for optimizing the application of absorbent, which explain the interaction between adsorbate molecules and adsorbent.

For the adsorption isotherm studies, the adsorption data of heavy metal ions and dye molecules were fitted to Langmuir (6) and Freundlich (7) equations, respectively.[30] The results were shown in Table 2.

$$\frac{C_e}{Q} = \frac{1}{K_L Q_{max}} + \frac{C_e}{Q_{max}} \tag{6}$$

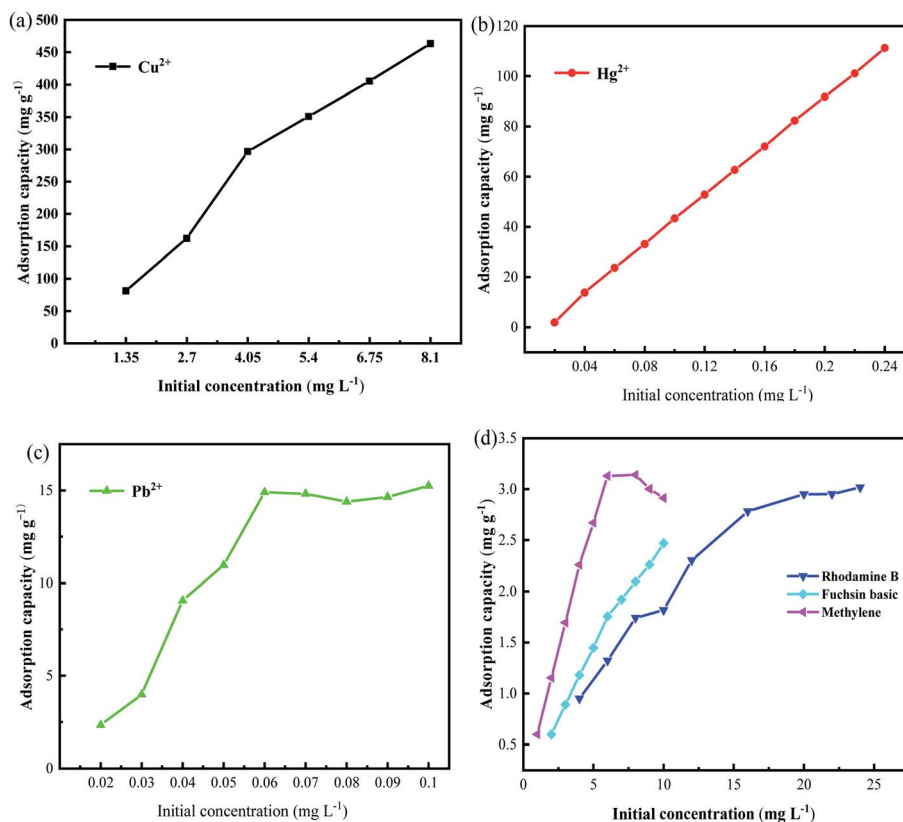**Fig. 3** Effect of initial concentration on adsorption at 30 °C.

Table 1 Parameters of kinetics model for adsorption of pollutants on CS@PDA@Fe$_3$O$_4$

Pollutants	Pseudo-first-order			Pseudo-second-order			Intraparticle diffusion	
	Q	K_1	R^2	Q	K_2	R^2	K_{int}	R^2
Cu^{2+}	784.15	0.145	0.8746	416.67	0.0032	0.9999	57.404	0.9255
Hg^{2+}	9.16	0.032	0.9622	42.90	0.0035	1.0000	0.2349	0.9758
Pb^{2+}	2.63	0.048	0.8657	12.48	0.0400	0.9999	0.1563	0.9909
MB	2.07	0.061	0.6893	2.99	0.1020	0.9993	0.0464	0.986
FB	1.24	0.043	0.9626	2.48	0.0550	0.9974	0.0789	0.9091
RhB	0.58	0.055	0.9130	3.08	0.1500	0.9997	0.0149	0.9531

$$\ln Q = \ln K_f + \frac{\ln C_e}{n} \qquad (7)$$

where C_e is the equilibrium concentration of metal ions in solution (mg L^{-1}), and Q is the equilibrium adsorption capacity (mg g^{-1}), Q_{max} (mg g^{-1}) and K_L (L mg^{-1}) are the Langmuir constant which is related to the adsorption capacity and energy of adsorption, respectively. K_f is the Freundlich constant related to adsorption capacity.
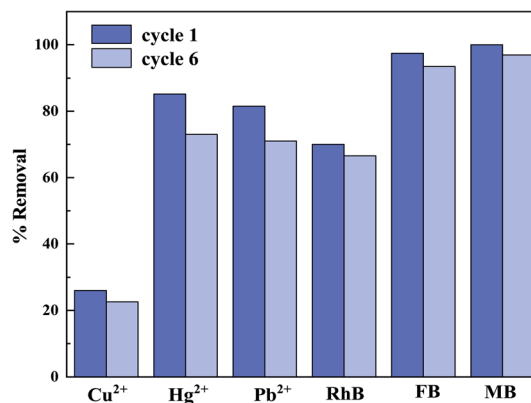
The R^2 of both fitting models is relatively high, and the R^2 of the Langmuir model is generally higher than that of the Freundlich model. This result indicates that the adsorption of pollutants on PDA/CS/Fe$_3$O$_4$ nano-sorbents occurred as a single monolayer, and the interaction force between metal ions can be ignored. Based on the theoretical analysis of the obtained data, the theoretical Q_{max} value of the nano adsorbent for Cu(II), Hg(II), Pb(II), MB, FB and RhB were respectively 909.0 mg g^{-1}, 94.0 mg g^{-1}, 20.2 mg g^{-1}, 3.6 mg g^{-1}, 2.4 mg g^{-1}, 2.9 mg g^{-1}, which was very close to the experimental data.

3.6 Desorption and reusability

Considering the cost in practical applications, it is necessary to study the analysis and regeneration of nano-adsorber. Desorption tests were studied to assess the regeneration and recycling of the CS@PDA@Fe$_3$O$_4$ nanocomposite regarding removing heavy metal ions and dye molecules *via* performing six adsorption/desorption cycles. It can be seen from Fig. 4 that the removal rate of nano-adsorber decreased slightly after the analysis operation with an ethanol solution, but it still has high removal efficiency.

Fig. 4 Desorption and reusability of CS@PDA@Fe$_3$O$_4$.

4. Conclusions

In this paper, a simple method is used to synthesize chitosan-grafted CS@PDA@Fe$_3$O$_4$ magnetic nano-adsorber with Fe$_3$O$_4$ as the magnetic core and PDA as the intermediate layer. These nano-adsorber membranes were utilized to eliminate the heavy metal ions (Cu(II), Hg(II), Pb(II)) and dye molecules (MB, FB, RhB) from aqueous solutions. The effects of static adsorption parameters such as pH, adsorbent concentration, metal initial concentration and time on adsorption performance were investigated. The results showed that the magnetic nano-adsorber had good adsorption performance and magnetic responsiveness. Besides, the experiment of desorption and regeneration proves that CS@PDA@Fe$_3$O$_4$ magnetic nano-adsorber can be recycled. This study has practical guiding significance for the treatment of pollutants in adsorbed water.

Conflicts of interest

There are no conflicts to declare.

Acknowledgements

Table 2 Parameters of isotherm model for adsorption of pollutants on CS@PDA@Fe$_3$O$_4$

Pollutants	Langmuir parameters			Freundlich parameters		
	K_L	Q_{max}	R^2	$\ln K_f$	N	R^2
Cu(II)	22.0	909.0	0.9759	9.2199	1.015	0.9713
Hg(II)	35.4	94.0	0.9868	5.246	2.70	0.9883
Pb(II)	165.0	20.2	0.9955	3.4434	5.50	0.9490
MB	0.4	3.6	0.9833	0.0565	2.416	0.9267
FB	12.3	2.4	0.9905	0.3238	5.214	0.9501
RhB	13.1	2.9	0.9287	0.4508	3.948	0.9465

References

1 M. A. Albakri, T. A. Saleh, Y. Mankour, T. F. Garrison and O. C. S. Al Hamouz, *J. Colloid Interface Sci.*, 2021, **582**, 428–438.

2 N. Ali, S. Uddin, A. Khan, S. Khan, S. Khan, N. Ali, H. Khan, H. Khan and M. Bilal, *Int. J. Biol. Macromol.*, 2020, **161**, 1305–1317.

3 V. Ball, D. Del Frari, M. Michel, M. J. Buehler, V. Toniazzo, M. K. Singh, J. Gracio and D. Ruch, *BioNanoScience*, 2011, **2**, 16–34.

4 A. R. Cestari, E. F. Vieira, A. A. Pinto and E. C. Lopes, *J. Colloid Interface Sci.*, 2005, **292**, 363–372.

5 C. Dumitriu, S. I. Voicu, A. Muhulet, G. Nechifor, S. Popescu, C. Ungureanu, A. Carja, F. Miculescu, R. Trusca and C. Pirvu, *Carbohydr. Polym.*, 2018, **181**, 215–223.

6 Y. Guan, H. Y. Yu, S. Y. H. Abdalkarim, C. Wang, F. Tang, J. Marek, W. L. Chen, J. Militky and J. M. Yao, *Int. J. Biol. Macromol.*, 2019, **132**, 51–62.

7 V. K. Gupta, P. J. M. Carrott, M. M. L. Ribeiro Carrott and Suhas, *Crit. Rev. Environ. Sci. Technol.*, 2009, **39**, 783–842.

8 C. Hou, H. Zhu, Y. Li, Y. Li, X. Wang, W. Zhu and R. Zhou, *Appl. Microbiol. Biotechnol.*, 2015, **99**, 1249–1259.

9 A. Khan, S. Badshah and C. Airoldi, *Colloids Surf., B*, 2011, **87**, 88–95.

10 A. Khan, S. Begum, N. Ali, S. Khan, S. Hussain and M. Sotomayor, *Water Sci. Technol.*, 2017, **75**, 2034–2046.

11 A. Khan, F. Wahid, N. Ali, S. Badshah and C. Airoldi, *Desalin. Water Treat.*, 2014, **56**, 1099–1109.

12 C. Lee and S. Y. Lee, *Colloids Surf., B*, 2015, **127**, 89–95.

13 Y. Liu, K. Ai and L. Lu, *Chem. Rev.*, 2014, **114**, 5057–5115.

14 Y. Liu and Y.-J. Liu, *Sep. Purif. Technol.*, 2008, **61**, 229–242.

15 C. Lobo, J. Castellari, J. Colman Lerner, N. Bertola and N. Zaritzky, *Int. J. Biol. Macromol.*, 2020, **164**, 1575–1583.

16 A. L. Popovic, J. D. Rusmirovic, Z. Velickovic, T. Kovacevic, A. Jovanovic, I. Cvijetic and A. D. Marinkovic, *J. Ind. Eng. Chem.*, 2021, **93**, 302–314.

17 A. K. Sharma, Priya, B. S. Kaith, N. Sharma, J. K. Bhatia, V. Tanwar, S. Panchal and S. Bajaj, *Int. J. Biol. Macromol.*, 2019, **124**, 331–345.

18 Y. Xie, C. Chen, X. Lu, F. Luo, C. Wang, A. Alsaedi and T. Hayat, *J. Hazard. Mater.*, 2019, **379**, 120786.

19 L. Yang, Y. Peng, C. Qian, G. Xing, J. He, C. Zhao and B. Lai, *Chemosphere*, 2021, **263**, 128120.

20 S. Yang, Y. Hou, S. Xiong, F. Chen, Y. Jiang, C. Pan, J. Tang and G. Yu, *Sep. Purif. Technol.*, 2021, **258**, 117986.

21 J. Ye, X. Cong, P. Zhang, E. Hoffmann, G. Zeng, Y. Liu, W. Fang, Y. Wu and H. Zhang, *Appl. Surf. Sci.*, 2015, **356**, 128–134.

22 S. Zhang, Y. Zhang, G. Bi, J. Liu, Z. Wang, Q. Xu, H. Xu and X. Li, *J. Hazard. Mater.*, 2014, **270**, 27–34.

23 X. Xin, Q. Wei, J. Yang, L. Yan, R. Feng, G. Chen, B. Du and H. Li, *Chem. Eng. J.*, 2012, **184**, 132–140.

24 X. Li, Y. Qi, Y. Li, Y. Zhang, X. He and Y. Wang, *Bioresour. Technol.*, 2013, **142**, 611–619.

25 X. Guo, X. Du, Q. Wei, J. Yang, L. Hu, L. Yan and W. Xu, *J. Hazard. Mater.*, 2014, **278**, 211–220.

26 L. Zhou, Y. Wang, Z. Liu and Q. Huang, *J. Hazard. Mater.*, 2009, **161**, 995–1002.

27 W. Lee, J. U. Lee, B. M. Jung, J.-H. Byun, J.-W. Yi, S.-B. Lee and B.-S. Kim, *Carbon*, 2013, **65**, 296–304.

28 Y. Wang, Y. Zhang, C. Hou and M. Liu, *J. Taiwan Inst. Chem. Eng.*, 2016, **61**, 292–298.

29 X. Liu and D. J. Lee, *Bioresour. Technol.*, 2014, **160**, 24–31.

30 L. Hadjittofi, M. Prodromou and I. Pashalidis, *Bioresour. Technol.*, 2014, **159**, 460–464.